IOPscience iopscience.iop.org

Home Search Collections Journals About Contact us My IOPscience

Direct high-resolution determination of vacancy-type defect profiles in ion-implanted silicon

This article has been downloaded from IOPscience. Please scroll down to see the full text article.

2005 J. Phys.: Condens. Matter 17 S2323

(http://iopscience.iop.org/0953-8984/17/22/021)

View the table of contents for this issue, or go to the journal homepage for more

Download details:
IP Address: 129.252.86.83
The article was downloaded on 28/05/2010 at 04:55

Please note that terms and conditions apply.

INSTITUTE OF PHYSICS PUBLISHING JOURNAL OF PHYSICS: CONDENSED MATTER

J. Phys.: Condens. Matter **17** (2005) S2323–S2330 doi:10.1088/0953-8984/17/22/021

Direct high-resolution determination of vacancy-type defect profiles in ion-implanted silicon

P G Coleman[1], **R E Mason**[1], **M Van Dyken**[2] **and A P Knights**[2]

[1] Department of Physics, University of Bath, Bath BA2 7AY, UK
[2] Department of Engineering Physics, McMaster University, Hamilton, ON, L8S 4L, Canada

E-mail: p.g.coleman@bath.ac.uk

Received 6 October 2004
Published 20 May 2005
Online at stacks.iop.org/JPhysCM/17/S2323

Abstract
The depth distribution of open-volume point defects created by room temperature implantation of Cz silicon by 100 keV B^+ ions at a dose of 5×10^{14} cm^{-2} has been determined by enhanced-resolution beam-based positron annihilation spectroscopy (PAS). By incremental controlled etching (via anodic oxidation of 50–100 nm layers) the depth resolution of the PAS is maintained at ∼50 nm by using positrons implanted at energies below 2 keV to probe each layer as it brought close to the surface by the etching process. The etch depths have been verified by using secondary-ion mass spectrometry to profile the boron depth distribution. The results are in good agreement with Monte Carlo simulations, particularly in the traditionally difficult-to-measure deep tail region.

1. Introduction

Variable-energy (beam-based) positron annihilation spectroscopy (VEPAS) has for two decades been applied successfully to the non-destructive study of open-volume point defects in thin films and in the first few microns beneath the surface of solids [1]. The most common form of VEPAS is based on the Doppler broadening of the 511 keV annihilation line; the extent of the broadening is determined by the momentum distribution of the annihilated electrons, which is in turn determined by the annihilation state. The broadened linewidth is typically described by the sharpness parameter S, a single number equal to the ratio of the central part of the annihilation line to the total area. Hence if the average electron momentum is lower in an annihilation site than in the bulk, as is often the case in a vacancy-type defect, the Doppler broadening will be less, the annihilation line sharper and the S parameter value higher.

Control of the energy of the implanted positrons, typically between 0.5 and 30 keV, allows one to gain some semi-quantitative information non-destructively on the depth profile of the

 © 2005 IOP Publishing Ltd Printed in the UK

defects. This information is usually obtained through fitting raw positron data with a code such as VEPFIT [2], which assumes a Makhovian positron implantation profile

$$P(z, E) = -\frac{\mathrm{d}}{\mathrm{d}z}\{\exp[z/z_0]^m\} \tag{1}$$

where z is the distance measured from the surface, E is the incident positron energy and z_0 is related to the mean implantation depth $\bar{z}$ for a material of density ρ and is commonly given by $(40/\rho)E^{1.6}$ (z_0 in nm and E in keV). The most widely accepted version of equation (1) uses $m = 2$—i.e., $P(z, E)$ is a Gaussian derivative, for which $z_0 = 1.11\bar{z}$. VEPFIT then solves the positron diffusion equation and calculates a positron annihilation depth profile which best fits the observed data $S(E)$ by fitting values for the S parameter and the effective positron diffusion length L_{eff} in each of any number of layers whose boundaries can either be fixed or fitted. For the simplest case of ion-implanted silicon, VEPFIT will fit the raw data by assuming a simple defect box profile of fitted thickness having characteristic values of S and L_{eff}. Average defect concentrations C_{D} can be deduced from L_{eff} if the specific trapping rate ν and the mean positron lifetime in pure Si, λ, are known:

$$L_{\mathrm{eff}} = L_{+}[\lambda/(\lambda + \nu C_{\mathrm{D}})]^{1/2} \tag{2}$$

and from the average S if S values characteristic of all the annihilation sites present are known. For example, if the only two possible annihilation sites are a divacancy and bulk Si, with normalized S values of 1.04 and 1.00, respectively, then

$$C_{\mathrm{D}} = (\lambda/\nu)(S - 1)/(1.04 - S). \tag{3}$$

The two routes to C_{D} should be consistent. The more complicated the defect profile is, the more unreliable the fitting results become; generally it is wise to accept the simplest model for which a good fit can be obtained, and so one obtains only an indication of the average depth of the defect distribution and its average S parameter. In addition, the width of the positron depth profile is similar to the mean depth probed, and hence resolution deteriorates with depth and information on deep-lying defects (such as buried layers) is unreliable.

Damage profiling by VEPAS with approximately constant depth resolution, achieved normally only at low implantation energies E, can be performed if the non-destructive nature of the standard spectroscopy is abandoned and the sample is progressively etched to bring successive parts of the defect distribution close to the surface. This concept—valid only if the etching does not itself introduce appreciable new damage—is illustrated schematically in figure 1. After etching, the shaded layer of defects is at the surface and a narrow distribution of positrons can be implanted into it, whereas without etching the same layer—now buried—it can only be reached by high-energy positrons which have a very broad implantation profile; only a small fraction of the implanted positrons stop in the layer of interest, and the VEPAS response is considerably smeared as a consequence. Thus the narrow $P(z, E)$ is maintained across the entire damage profile. The principle of enhanced-depth-sensitivity VEPAS has been discussed by Knights, Coleman and co-workers [3–5] and by Krause-Rehberg *et al* [6], and applied by Knights *et al* [7], Malik *et al* [8] and Janson *et al* [9] to study deep defect tails, Simpson *et al* [10] to study damage caused by ions implanted through a SiO_2 layer, Fujinami *et al* to study damage in He-implanted Si [11], Saarinen *et al* and Kauppinen *et al* to study vacancy distributions in In-implanted GaAs and MeV proton-implanted Si [12, 13] and Krause-Rehberg *et al* [14–16] to study damage caused by sawing GaAs wafers and impurity gettering at half-ion range in self-implanted silicon. In [7] and [8] simple one- or two-step etching was performed using anodic oxidation as an intermediate stage (as discussed later). In [9] etching was performed using an inductively coupled plasma system. In [10–13] direct chemical etching was employed. In [14] *in situ* ion sputtering was used progressively to remove

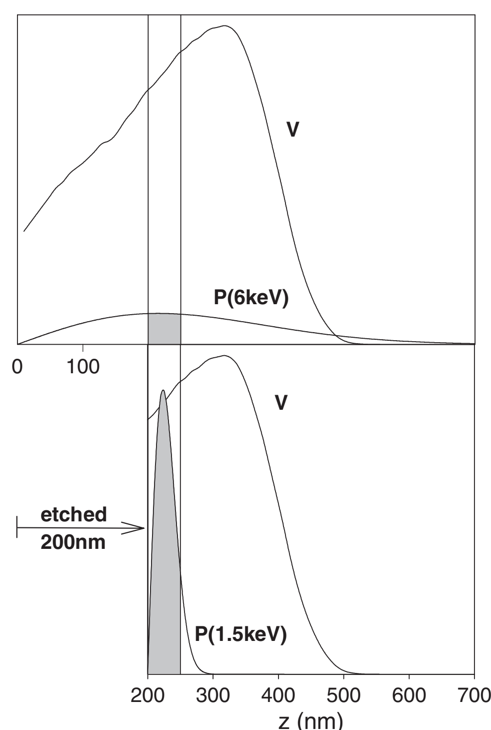

Figure 1. Example of interrogation of defects at depths z in the region 200–250 nm below the surface. Top: non-destructive (standard) method—peak sensitivity with incident positron energy $E = 6$ keV (FWHM of the positron implantation profile $P \sim 350$ nm). Bottom: etch-and-measure method—over 90% of 1.5 keV positrons are implanted into the defect region after 200 nm etched (FWHM ~40 nm).

surface layers. In [6] and [16] a 1 μm diameter positron microbeam was used to scan across a wedge-shaped piece (cut angle $\sim 1°$) of ion-implanted silicon.

Widely used codes such as TRIM [17] calculate vacancy depth profiles, but do not account for post-implantation migration and agglomeration. For example, earlier VEPAS measurements have confirmed that at room temperature only a few per cent of the original vacancies survive, and then in the form of divacancies. This paper describes in detail the method underlying enhanced-depth-sensitivity VEPAS and the first experimental results obtained for ion-implanted silicon. Secondary-ion mass spectrometry (SIMS) has been performed on the same samples, and advanced simulations have been performed which account for the crystalline nature of the sample and hence ion channelling during implantation.

2. Sample preparation

Samples of Cz Si were implanted with 100 keV boron ions at a dose of 5×10^{14} cm^{-2}. Each sample was then etched progressively via anodic oxidation; the (commonly used) technique is described in some detail in [4]. In summary, a voltage is applied between a sample (with native oxide removed) and a cathode, both mounted in a constantly stirred electrolyte of 90% ethylene glycol, 0.4% KNO_3 and 10% water. The current density is approximately 12.5 mA cm^{-2}. The electrolyte is illuminated to enhance the anodic reaction. The oxide growth is dependent on the applied potential; growth ceases when the oxide thickness is such that the current essentially

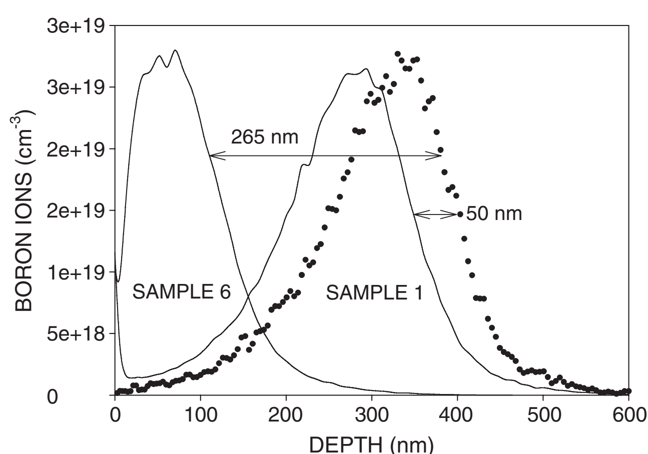

Figure 2. SIMS profiles for boron ions for 53 nm and 261 nm etch depths, together with the simulated profile. The equivalent etch depths suggested by these profiles are 50 and 265 nm, respectively, which agree with the measured etch depths to within the uncertainties in measurement.

ceases to flow. For example, about 40 nm of oxide is grown for a potential difference of 75 V. The oxide thickness is measured by ellipsometry, and typically varies by only a few per cent across a sample surface. The oxide thus grown is then etched off by dilute hydrofluoric acid, and the procedure repeated as many times as required. The thickness of Si removed was calculated by multiplying the oxide thickness by 0.31, a factor obtained by (a) direct post-etch step measurement and (b) SIMS measurements of the boron profiles after etching (see below).

That no VEPAS-detectable damage was introduced by this process was checked by taking measurements on an unimplanted Si sample.

The set of ten samples created in this way had the following thicknesses of material etched off (in nm, uncertainties in parentheses): 53.3 (1.0), 90.0 (1.4), 132.0 (1.7), 178.7 (11.6), 208.8 (4.0), 260.6 (2.2), 294.0 (3.9), 377.6 (3.6), 460.8 (16.6) and 544.4 (3.0). These etch depths were confirmed by direct step measurement and by SIMS profiles of the implanted boron ions (figure 2). We shall refer to these samples by the numbers 1–10.

3. Results and data analysis

The raw VEPAS data for the unetched and unimplanted samples are shown in figure 3. The increase in the value of the lineshape parameter S indicates the presence of open-volume point defects below the surface; the asymptotic value at high incident positron energies is the value for undamaged bulk Si. Both data sets exhibit the lower S parameter characteristic of annihilation events at or near the sample surface. The VEPFIT result for the implanted sample is obtained by assuming a simple box defect profile of thickness 540 nm with an average S value of 1.041 and $L_{\mathrm{eff}} = 23$ nm. Using equation (2) with $L_{+} = 250$ nm the average concentration of defects in this layer was calculated to be 5.3×10^{-4} per atom. The route to C_{D} via S is unavailable here as the trapping is essentially saturated and the value of S is that of the divacancy in Si (this is consistent with the high value of C_{D} obtained from L_{eff}). This simple analysis demonstrates the limitations of VEPFIT in depth profiling.

We now turn to the etched samples. The raw VEPAS data, together with VEPFIT results, are shown in figure 4. Data for samples 2, 4 and 6 are omitted to aid clarity. The depth of

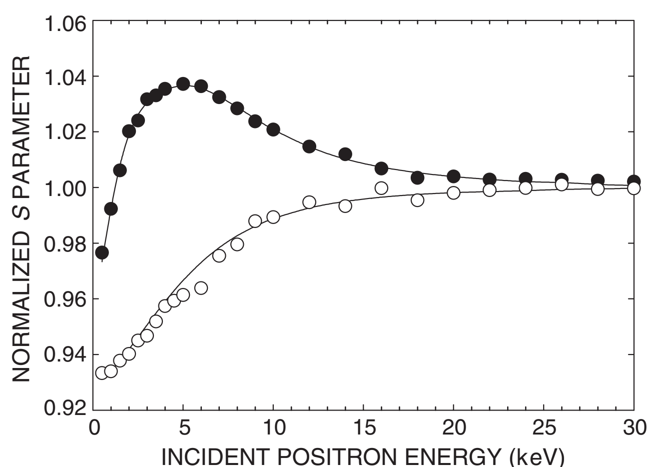

Figure 3. Raw VEPAS data $S(E)$, normalized to the value of S for bulk Si, for unimplanted Si and Si implanted with 100 keV boron ions at a dose of 10^{14} cm^{-2}. The solid lines are fits to the data using the code VEPFIT.

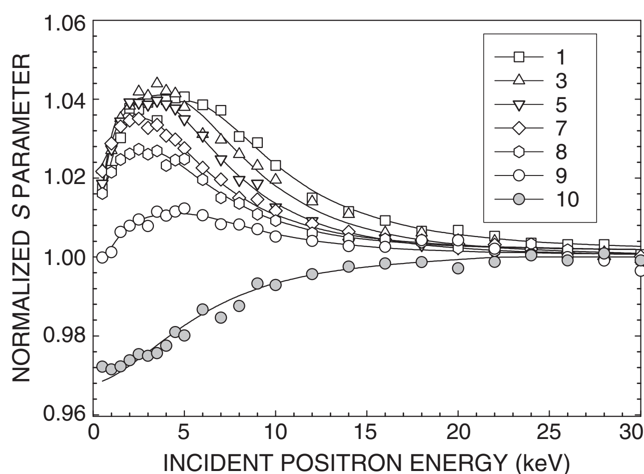

Figure 4. Normalized raw VEPAS data $S(E)$ for etched samples 1–10 (data for samples 2, 4 and 6 not shown to aid clarity). Solid lines are VEPFIT fits to the data for samples 1–9; the solid line under data for sample 10 is a fit to data for unimplanted Si.

the damage box profiles given by VEPFIT decrease in accordance with the etch depths for samples 1–7 (again with the saturated defect S value of 1.04), and a deeper tail of defects is revealed for samples 8 and 9—i.e., beyond 540 nm. One feasible method for obtaining the full defect profile is thus as follows: (a) set up ten layers corresponding to the etch depths, (b) fit the defect profile for layer 10—i.e. for the most etched sample, (c) fix the parameters for layer 10 and fit the profile for layers 9 and 10—i.e. for the sample 9 data, (d) repeat this procedure until sample 1 is reached, each time fixing the parameters obtained from the previous analysis. This procedure is reasonable for samples which do not exhibit saturation positron trapping; however, this is not the case here, and reliance on diffusion lengths from VEPFIT to yield defect concentrations in a multilayered sample is not advisable.

Instead we use the VEPAS data corresponding to positron annihilation in the top layer of each sample—to a depth defined by the next etch depth—as suggested by figure 1. Diffusion to a different S value at the surface allows us to compute near-surface defect concentrations which, if deeper in the material, would trap all the positrons. Although diffusion to the surface is the key to the analysis method described herein, there are two interrelated problems with using data in this region. First, significant diffusion to the surface—with consequent annihilation there with a lower S parameter—requires precise knowledge of the surface S value. Second, when positrons are implanted at energies below 1 keV there is a significant probability that they are not thermalized and return to, and penetrate, the surface [18]; should this happen then they may form positronium [19] and decay with a different S parameter, distorting the data obtained. This distortion also makes determination of the true surface S value more difficult. The effects of these near-surface problems are minimized by (a) using data for positron energies of 0.5, 1.0, 1.5 and 2.0 keV—i.e. only one datum which may be corrupted by significant epithermal positron effects, (b) evaluating the surface S value by extrapolation from higher energies and (c) weighting more heavily those data points for which there is less diffusion to the surface and thus less uncertainty in the derived defect concentration values.

The analysis method is summarized as follows. The assumption is first made that we are able to model the defect profile as a series of ten boxes, each of thickness determined by successive etch depths; for each box layer we assume a constant defect concentration. For each sample the box we study corresponds typically to the first 50 nm or so.

The S parameter at each incident energy is a linear combination of contributions from annihilations at the surface (S_S), in defects (S_D) and in the bulk (S_B):

$$S = F_S S_S + F_D S_D + F_B S_B \tag{4}$$

where F_i is the fraction of positron annihilated in state i, where $\sum_i F_i = 1$. The surface fraction F_S for an incident positron energy E is computed from

$$F_S = \int_0^\infty P(z, E) \exp(-z/L_{\mathrm{eff}})\, \mathrm{d}z, \tag{5}$$

the defect fraction F_D from

$$F_D = \nu C_D(1 - F_S)/(\nu C_D + \lambda) \tag{6}$$

and $F_B = 1 - F_S - F_D$. Each fraction F_i therefore depends on the energy E.

The next step is to calculate values for the effective positron diffusion length L_{eff} for a wide range of C_D values, using equation (2). Then, using each pair of L_{eff} and C_D values, the three fractions F_i are computed using the expressions above for each energy E. Finally, using a value for S_S found by extrapolating $S(E)$ from 1–3 keV to $E = 0$, and values of 1.04 and 1.00 for S_D and S_B, respectively, a value for the average S at each energy E is found via equation (4). Values of C_D (and thus also L_{eff}) for which the computed S equals the measured S at each energy E are recorded; the weighted mean of C_D for the three or four values of E corresponding to implantation into the first 50–100 nm (depending on the etch depth) is the value taken for the near-surface box layer. This procedure is repeated for each of the ten samples.

The final adjustment to the C_D value is a first-order correction which allows for diffusion into the second layer. This is done by computing the fraction f_2 of positrons implanted into the top layer which diffuse into the second layer, using a version of equation (5) with the surface replaced by the interface between the two layers. (The correction is small when C_D is high and L_{eff} correspondingly small.) C_D for layer 1, C_{D1}, is corrected to $C'_{D1} = (C_{D1} - f_2 C_{D2})/(1 - f_2)$.

The final values for C'_{Dn} are, as discussed earlier, average values over the etch depths (which are mostly ∼50–80 nm wide). Rather than present the data as a raw histogram, we have instead

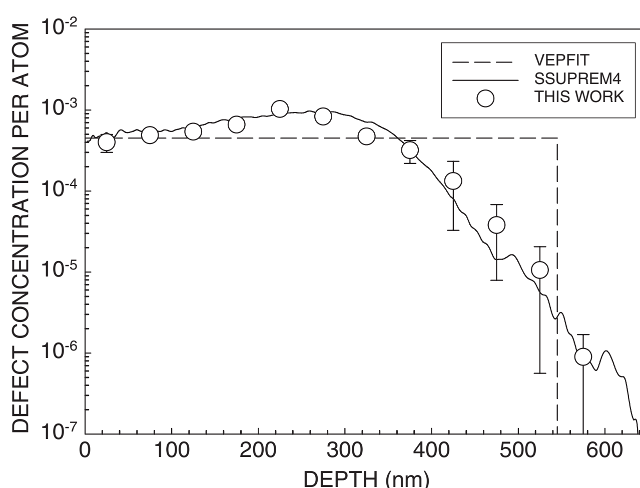

Figure 5. Defect concentration profile obtained from this work, the simple VEPFIT box profile and the SSUPREM4 simulation scaled down by a factor of 0.125. Error bars result from the weighted averaging and where not visible are within data points.

calculated defect concentrations at 50 nm intervals by taking weighted contributions from the appropriate depth ranges. The final results of this analysis are presented in figure 5.

The data agree reasonably well with simulations of vacancy damage using the SSUPREM4 code [20], which simulates channelling but not post-implant vacancy migration or agglomeration. The simulation results have been scaled down by a factor of 8. It is particularly satisfying to note the good agreement between the shape of the simulation and the present measurements in the deep-lying tail of the distribution, over a range of three orders of magnitude.

The similarity of the monovacancy distribution predicted by simulation and the observed distribution—expected to be primarily divacancies—is probably a result of the high migration energies of divacancies in Cz Si. Further work is under way to compare defect profiles in Cz with those in float-zone and epitaxially grown Si implanted under similar conditions. The experimental technique and analysis procedure will be honed in the light of the experience gained in this pilot study, and it is hoped that new information on the migration of vacancy-type defects in the three types of Si sample will be gained, especially in the deep tail regions.

Acknowledgments

The authors acknowledge the EU CADRES project for financial support for attendance at the workshop at which this work was presented. We are grateful to Dr R M Gwilliam of the University of Surrey Ion Beam Centre, UK, for ion implantation. The SIMS was carried out at Surface Science Western, University of Western Ontario. This work was supported in part by the Natural Sciences and Engineering Research Council of Canada (NSERC).

References

[1] Coleman P G (ed) 2000 *Positron Beams and their Applications* (Singapore: World Scientific)
[2] van Veen A, Schut H, de Vries J, Hakvoort R A and Ijpma M R 1990 *AIP Conf. Proc.* **218** 171
[3] Knights A P, Nejim A, Barradas N P and Coleman P G 1999 *Nucl. Instrum. Methods* B **148** 340

[4] Coleman P G and Knights A P 1999 *Appl. Surf. Sci.* **149** 82
[5] Knights A P and Coleman P G 2000 *Defect Diffus. Forum* **183–5** 41
[6] Krause-Rehberg R, Börner F, Redmann F, Egger W, Kögel G, Sperr P and Triftshäuser W 2002 *Appl. Surf. Sci.* **194** 210
[7] Malik F, Coleman P G, Knights A P, Gwilliam R, Nejim A and Ho O Y 1998 *J. Phys.: Condens. Matter* **10** 10403
[8] Knights A P, Nejim A, Coleman P G, Kheyrandish H and Romani S 1998 *Appl. Phys. Lett.* **73** 1373
[9] Janson M S, Slotte J, Kuznetsov A Yu, Saarinen K and Hallen A 2004 *J. Appl. Phys.* **95** 57
[10] Simpson P J, Spooner M, Xia H and Knights A P 1999 *J. Appl. Phys.* **85** 1765
[11] Fujinami M, Miyagoe T, Sawada T, Suzuki R, Ohdaira T and Akahane T 2003 *Phys. Rev.* B **68** 165332
[12] Saarinen K, Hautojärvi P and Corbel C 1998 *Identification of Defects in Semiconductors* ed M Stavola (New York: Academic) p 42
[13] Kauppinen H, Corbel C, Skog K, Saarinen K, Laine T, Hautojärvi P, Desgardin P and Ntsoenzok E 1997 *Phys. Rev.* B **55** 9598
[14] Börner F, Eichler S, Polity A, Krause-Rehberg R, Hammer R and Jurisch M 1999 *Appl. Surf. Sci.* **149** 151
[15] Krause-Rehberg R, Börner F and Redmann F 2000 *Appl. Phys. Lett.* **77** 3932
[16] Krause-Rehberg R, Börner F, Redmann F, Gebauer J, Kögler R, Kliemann R, Skorupa W, Egger W, Kögel G and Triftshäuser W 2001 *Physica* B **308–10** 442
[17] Ziegler J F, Biersack J P and Littmark U 1985 *The Stopping and Range of Ions in Solids* (New York: Pergamon)
[18] Knights A P and Coleman P G 1996 *Surf. Sci.* **367** 238
[19] Howell R H, Rosenberg I J and Fluss M J 1986 *Phys. Rev.* B **34** 3069
[20] 2003 *SSUPREM4* provided by Silvaco International